All-Sky High Frequency Search for Burst Gravitational Waves in the First Joint Science Run by LIGO and Virgo
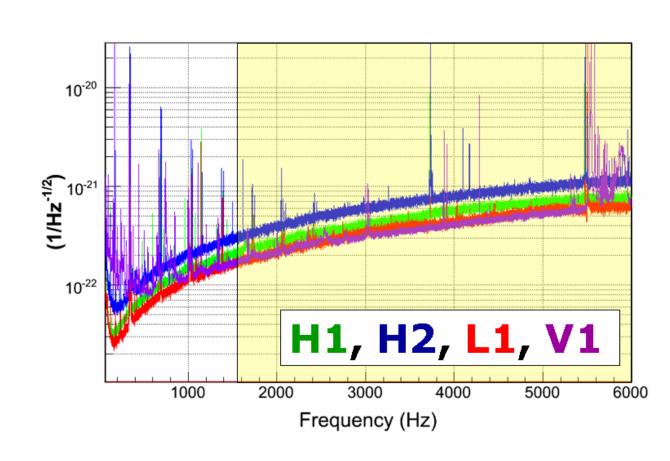
Marco Drago for the LSC and Virgo Collaboration

Department of Physics, University of Padova, Italy

Abstract

The first long term observation by the LIGO-Virgo network of gravitational wave detectors occurred in 2007. This was a unprecedented opportunity to search for transient gravitational waves with a network configuration of three different sites in the higher frequency band, where the detectors shared similar spectral sensitivities. Since the detectors have different directional sensitivities, the full potential of such a network can be achieved by a coherent method of data analysis. In this poster, we present a detailed look of the coherent search method for transient gravitational wave signals at frequencies from 1.3 up to 6 kHz during the joint LIGO-Virgo observation. We focus on the methodological issues for the analysis of this data set, highlighting the performances of the network with respect to false alarm and detection efficiency.

Introduction

▸ **Scientific Goals:** This search for burst gravitational waves is targeted to transient signals of short duration ($\leq$ s) in the higher frequency bandwidth of the LIGO and Virgo detectors, from 1280 to 6000 Hz. It complements the standard lower frequency burst search performed by the LIGO-Virgo network (64 − 2000 Hz). The frequency overlap of the searches preserves the detection efficiency for possible signals at in-between frequencies and is useful as well to test the newer high frequency search against the standard one. The upper frequency bound is set at 6 kHz by the calibration systematic uncertainties of LIGO detectors. Target gravitational wave sources include: NS instabilities and vibrational modes [6], NS-NS mergers and post-merger phases ([3],[4],[5]), BH-BH mergers and BH ring-downs when BH mass is $\leq 8M_\odot$ [8], SuperNovae core collapses emitting at high frequencies [10]. The horizon of this observation is likely limited to Galactic sources, apart from the binary mergers.

Figure: 1

DETECTORS	OBSERVATION TIME [d]	
H1 H2 L1 V1	68.1	72.3 3-sites
H1 L1 V1	4.2	
H1 H2 L1	122.5	138.1 2-sites
H1 H2 V1	15.6	
H1 H2	35.6	

Tab.1 : configurations of detectors and analyzed observation time in S5Y2-VSR1

▸ **Data Set:** The three LIGO detectors and the Virgo detector showed similar spectral sensitivities in 2007 (see Fig.1), where the dominant contribution came from the shot noise of the Laser light. The analysis has been performed on the data of the second calendar year of the LIGO 5th Science Run (S5y2, from Nov. 2006) and the first Science Run of Virgo (VSR1, from May 18th 2007). The joint observation ended on Oct.1st 2007 (see Tab.1 for exclusive livetimes). The observation time was subdivided in disjoint subsets, each one corresponding to the simultaneous observation by a specific network configuration. We performed separate analyses per each network configuration with at least two detectors and observation time greater than a few days (see Tab.1). In particular, for the first time we had available about 72 days of simultaneous observations by three detector sites.

Methodology

▸ **Coherent Search:**

The differences in directional sensitivities of the detectors makes them sensitive to different combinations of the two GW polarization amplitudes (especially between Virgo and the LIGO detectors). The data analysis methodology should take care of the fact that the detector responses to the same GW are different in amplitude for most sky locations. Therefore an analysis based on a straightforward correlation of the detectors data is not granted to work any more. Moreover the differences in spectral sensitivities of the detectors have to be taken into account. The methodology used by coherent WaveBurst ([1],[2]) is based on the maximization of the likelihood ratio with respect to the GW parameters (polarization amplitudes and direction), where the likelihood is estimated summing coherently detectors data $x_k[i]$ and detector responses $\xi[i]$. The method does not make assumptions on the GW polarization amplitudes vs time, but of course the search is practically limited to a part of the duration-frequency space. Data from N detector are combined to calculate the Likelihood Ratio:

$$L = \Sigma_i \Sigma_{k=1}^N \frac{1}{\sigma_k} \left[x_k^2[i] - (x_k[i] - \xi_k[i])^2 \right]$$

(σ=detector variance, x=data vector, $\xi = h_+ F_+ + h_\times F_\times$=detector response, k=detector index, i=datum index) The solution $h = (h_+, h_\times)$ that gives the maximum Likelihood Ratio is our estimate of the GW.

To grasp a feeling of what the maximization of the likelihood ratio means, consider three misaligned detectors: per each tentative sky direction the vector of the data of each detector x_k can be projected in two components related to a possible GW response and one component orthogonal to the previous ones, called the Null (see Figure: 2). In this representation the Likelihood ratio is simply the total energy of the data vector (i.e. $\|x_k/\sigma_k\|^2$) minus the energy of the Null (i.e. $\|(x - \xi)/\sigma_k\|^2$) and its maximization over the sky directions automatically identifies candidate events caracterized by a higher energy and a lower Null, therefore suppressing network excitations not compatible with a GW effect such as instrumental glitches.
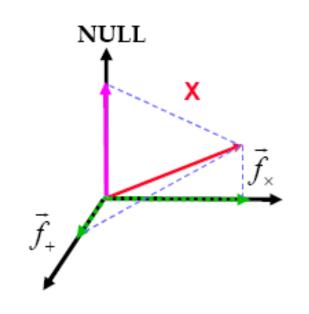

Figure: 2

▸ **Implementation details:**

The cWB pipeline uses wavelet layers at different time-frequency resolutions to be computationally efficient. In our analysis we used 6 resolution levels, 400Hz x 1/800 s, 200Hz x 1/400 s, ..., 12.5Hz x 1/25 s. The maximization of the likelihood ratio has been performed in the frequency range 1280-6000 Hz for wavelet pixels and clusters of pixels. The key test-statistics used to characterize the candidate events are:

Network correlation coefficient: $netcc = \frac{E_{cor}}{E_{cor}+N_{null}}$, E_{cor}=coherent energy, N_{null}=Null Energy

Effective correlated SNR: $\rho = \sqrt{\frac{E_{cor}cc}{N}}$ which roughly gives the typical signal to noise ratio per detector

Accidental Background and detection efficiency

▸ **Background estimation:**

For each detector configuration, experiment resamplings were performed by shifting the time series of one detector with respect to the others. For the V1H1L1 network, we shifted two detectors to increase the statistic. The time shifts were built with a step of 1.56 s up to a maximum shift of 300 s. For all the detectors networks, the resamplings obtained have then been separated in two sets at alternate shift number: one has been used for tuning the thresholds and the other for estimation of the False Alarm Rate (FAR) once the thresholds were chosen.
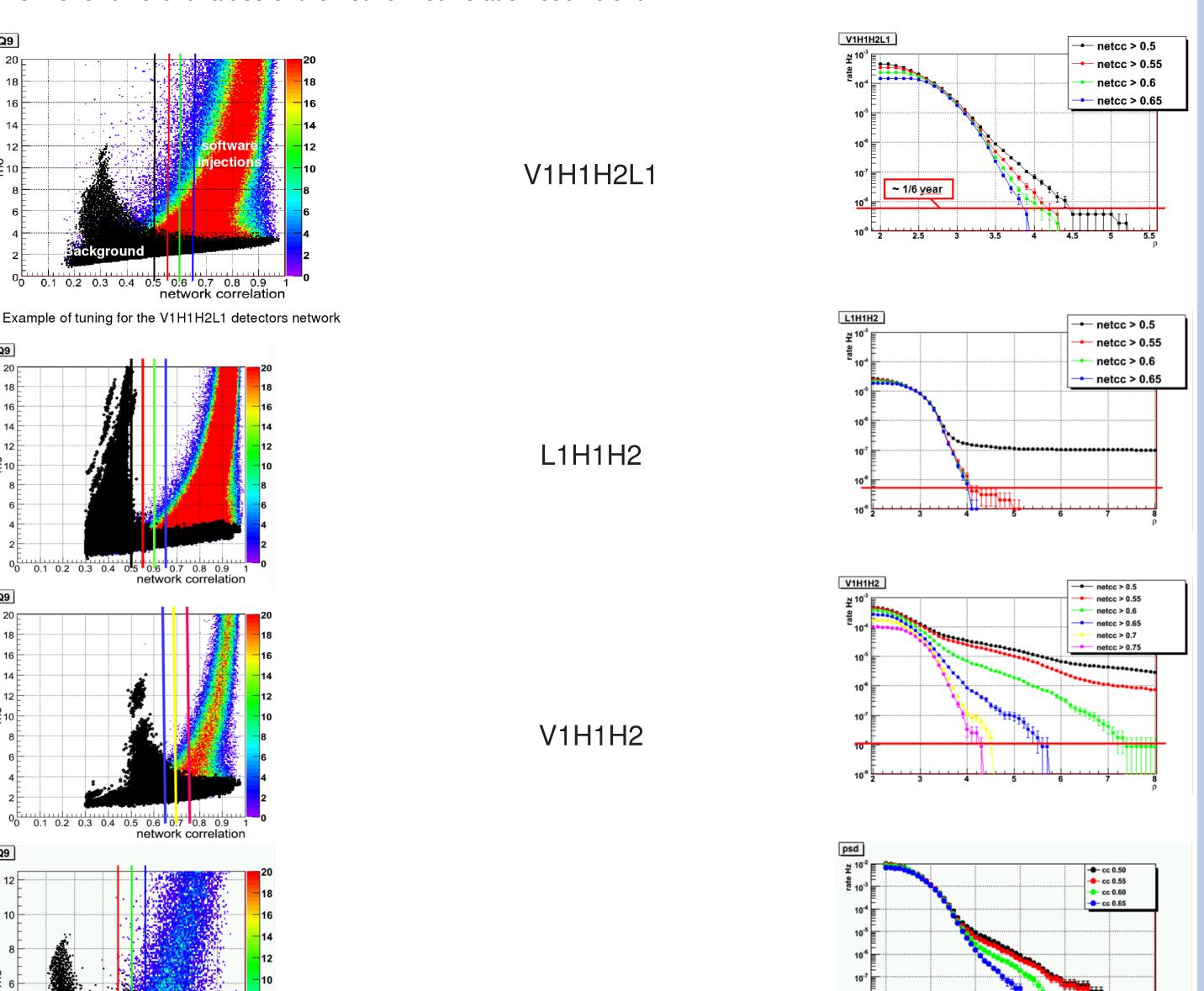
▸ **Detection Efficiency:**

it has been tested by injecting simulated signals into the data stream. In particular:

▸ SineGaussian Q9 (13 central frequencies) as an all-purpose testing set
▸ Sine Gaussian waveforms Q3 and Q100 linearly polarized to test sensitivity to shorter/longer waveforms
▸ White Noise Bursts with band/duration = 100 Hz / 0.01 s and 1000 Hz / 0.1 s as an extreme case test
▸ Ring down waveforms τ = 0.2 s linear and circularly polarized for NS f-modes related to SGR
▸ Numerical SN core collapse to BH, waveforms D1 and D4
▸ Ring Down Q9 linearly and circularly polarized to calibrate short Damped Sinusoids wrt SineGaussians
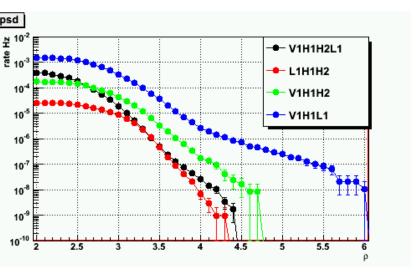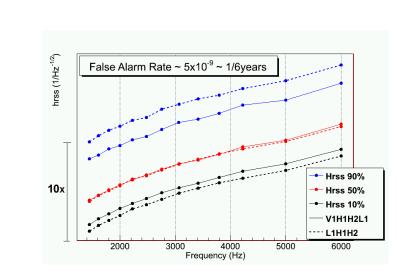
Tuning of the Analysis

▸ **Tuning:**

The thresholds on rho and Network Correlation Coefficient (netcc) have been tuned by seeking the best compromise between target FAR and preserving the detection efficiency. The target FAR has been set at about 1/6 years. Figures below show the scatter plot of background counts (black) and injections(colored) and the rate vs rho for different values of the network correlation coefficient.
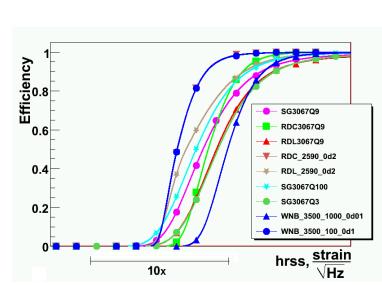

Example of tuning for the V1H1H2L1 detectors network

V1H1H2L1

L1H1H2

V1H1H2

V1H1L1

Background and Detection Efficincies at the tuned thresholds

▸ **Background**

▸ **Results: Detection efficiency estimates**

Detection efficiency varies for the different injection frequencies, scaling with detector sensitivity, as expected. Fig.8 show values of hrss at 10(black)-50(red)-90(blue)% efficiency for V1H1H2L1 (continuous line) and L1H1H2 (dashed line) networks at FAR $\approx$ 1/6 year. The asymptotical efficiency (hrss90%) results are better by a factor $\approx$ 40% for the network involving Virgo, due to the better sky coverage achieved with a 3rd site. For lower hrss injections (hrss10%), 3fold network is slightly better ($\approx$ 15%) due to the the threshold on rho being set an a slightly higher value for the 4fold configuration wrt the 3 fold at same FAR.

Calibration systematics

▸ **Calibration systematics:**

The effects of calibration systematic errors on the detection efficiency can be measured by Monte Carlo simulations , i.e. by injecting software signals in the network which are suitably deformed to mimic the mis-calibration at each detector. In real life the calibration comes with a mix of systematic and statistical uncertainties and their overall probability distribution represents our calibration ignorance. To get the best estimate of the detection efficiency, we perform a Monte Carlo in which each software injection is miscalibrated by drawing a new sample from the distribution of calibration uncertainty of that detector and frequency band. In other words, we marginalize the effects of the calibration uncertainties.

The typical increase in the GW amplitude corresponding to 50% efficiency is 5-12% for L1H1H2 and 3-8% for V1H1H2L1 (depending on the waveform central frequency).

A first order estimate of the uncertainty on the resulting estimate of the detection efficiency is estimated by performing a set of Monte Carlo simulations, each one using a fixed sample from the calibration uncertainty distribution per each detector-freq.band. To get an estimate of 1 sigma effect on the detection efficiency we performed 18 such Monte Carlo simulations.

Conclusions

References

[1] S. Klimenko et al., Phys. Rev. D 72 (122002) (2005).
[2] S. Klimenko et al., Class. Quantum. Grav., 25(11) (2008).
[3] L. Baiotti et al. Phys Rev. Lett. 99, 141101 (2007).
[4] L. Baiotti et al. Class. Quant. Grav. 24, S187 (2007).
[5] R. Oechslin and H.-T. Janka, Phys. Rev. Lett. 99, 121102 (2007).
[6] B.F. Schutz, Class. Quant. Grav. 16, A131 (1999).
[7] J.G. Jernigan, AIP Conf. Proc. 586, 805 (2001).
[8] K.T. Inoue and T. Tanaka, Phys. Rev. Lett. 91, 021101 (2003).
[9] J.E. Horvath, Modern Physics Lett. A 20, 2799 (2005).
[10] Baiotti et al., PRD 71, 024035 (2005)